A Novel Combination of Bevacizumab and Pembrolizumab Stimulates Tumour Immunity Through Vascular Normalisation in Humanised Mouse Model

Tianyun Qiao
Tangdu Hospital Fourth Military Medical University: Air Force Medical University Tangdu Hospital
Wenwen Guo
Yan'an University
Fancheng Meng
Tangdu Hospital Fourth Military Medical University: Air Force Medical University Tangdu Hospital
Yongsheng Zhou
Tangdu Hospital Fourth Military Medical University: Air Force Medical University Tangdu Hospital
Yanlu Xiong
Tangdu Hospital Fourth Military Medical University: Air Force Medical University Tangdu Hospital
Yangbo Feng
Tangdu Hospital Fourth Military Medical University: Air Force Medical University Tangdu Hospital
Caiqin Zhang
Fourth Military Medical University: Air Force Medical University
Yingtong Wu
Fourth Military Medical University: Air Force Medical University
Jinbo Zhao
Tangdu Hospital Fourth Military Medical University: Air Force Medical University Tangdu Hospital
Tao Jiang
Tangdu Hospital Fourth Military Medical University: Air Force Medical University Tangdu Hospital
Changhong Shi
Fourth Military Medical University: Air Force Medical University
Yong Han (hanyong_td@163.com)
Tangdu Hospital Fourth Military Medical University: Air Force Medical University Tangdu Hospital

---

Research

Keywords: Anti-programmed death 1, anti-vascular endothelial growth factor, humanised mouse model, immunotherapy, non-small cell lung cancer.

Posted Date: January 25th, 2021

DOI: https://doi.org/10.21203/rs.3.rs-152456/v1

Abstract

Background: Immunotherapy has dramatically changed the treatment landscape of cancer. Immunotherapies targeting the programmed death 1/programmed death ligand 1 pathway have been shown to lead to durable responses in patients with a variety of cancers. However, combination approaches are required to extend this benefit beyond a subset of patients. Studies have suggested that anti-angiogenic therapy can elicit or enhance tumor immunity response.Therefore, we hypothesised that combining immunotherapy with anti-angiogenic treatment may have a synergistic effect and may enhance the efficacy of both treatments.

Methods: We evaluated the combination of bevacizumab (anti-vascular endothelial growth factor monoclonal antibody) and pembrolizumab (anti-programmed death 1 monoclonal antibody) in two mouse models of human non-small cell lung cancer cell lines (H1299 and A549). We monitored tumour growth and examined changes in the tumour vasculature, along with the frequency and phenotype of tumour-infiltrating lymphocytes.

Results: The combination of bevacizumab and pembrolizumab synergistically inhibited tumour growth *in vivo* without overt toxicity in both cell lines. Combination therapy reprogrammed the immune microenvironment by increasing CD8+ cytotoxic T cell infiltration, thereby turning tumours with different phenotypes into inflamed (‘hot’) tumours. This is potentially mediated by vascular normalisation and endothelial cell activation, as demonstrated by a reduction in the number of microvessels and an increase in adhesion molecules.

Conclusions: Taken together, our preclinical studies demonstrate that the combination of bevacizumab and pembrolizumab had a synergistic anti-tumour effect and provides a theoretical basis for translating basic research into clinical applications.

Background

Lung cancer is the malignancy with the highest morbidity and mortality rates worldwide [1]. Non-small cell lung cancer (NSCLC) accounts for approximately 85% of all lung cancer cases, with a 5-year overall survival rate of approximately 15%. The majority of patients diagnosed with NSCLC have advanced-stage disease and are unsuitable for curative surgery [2]. The development of immune checkpoint inhibitors (ICIs) has ushered in a new era in the treatment of NSCLC, following the era of chemotherapy and targeted therapy [3]. ICIs are monoclonal antibodies targeting immune checkpoints, such as cytotoxic T lymphocyte-associated protein 4, programmed death 1 (PD-1), and programmed death ligand 1 (PD-L1) [4]. ICIs are designed to optimise the host’s immune response against tumour cells by increasing T cell cytotoxicity and suppressing tumour growth. The clinical application of a variety of ICIs has led to dramatic changes in the treatment strategy for patients with NSCLC [5]. However, the fact that only a small subset of patients with specific tumour types can benefit from ICIs limits their application. It has been reported that only tumours with pre-existing immunity (i.e., many tumour-infiltrating lymphocytes,

dense CD8 + T cells, and PD-L1 expression) respond well to ICIs. Other phenotypes, such as immune excluded tumours (immune cells only present at the periphery) and 'cold' tumours (little or no immune cell infiltration), respond poorly to single-dose ICIs [6]. However, the infiltration of most NSCLCs is characterised by immune exclusion [7]. Therefore, a suitable combination therapy is needed for increase the infiltration of tumour antigen-specific T cells in malignant tumour tissues, and then combined with ICIs to reverse tumour-induced immunosuppression and destroy tumour cells [8].

Angiogenesis contributes to tumorigenesis, tumour progression, and metastasis in numerous human malignancies [9]. In tumour tissues, a variety of transcription factors called hypoxia-inducible factors regulate the expression of angiogenic factors, including vascular epithelial growth factor (VEGF) and platelet-derived growth factor [10]. VEGF is the main regulator of angiogenesis. It stimulates the proliferation, migration, and neovascularisation of vascular epithelial cells by binding to VEGF receptors (VEGFRs) [11]. However, although the tumour has a rich blood supply, abnormal neovascularisation (stiffness, distortion, dilatation, and structural abnormalities) and low pericyte coverage leads to insufficient blood perfusion and increased vascular permeability. This reduces the supply of oxygen and nutrients, resulting in a microenvironment with high osmotic, hypoxic, acidic, and interstitial pressure [12]. The VEGF pathway not only regulates tumour vascularisation but also contributes to an inhibitory immune microenvironment, thereby enabling tumour cells to evade host immune surveillance [13]. Abnormal VEGF expression prevents the trafficking of tumour-reactive T cells to the tumour by inhibiting the expression of adhesion molecules in endothelial cells, specifically intercellular adhesion molecule 1 (ICAM-1) and vascular cell adhesion molecule 1 (VCAM-1) [14].

Anti-angiogenic drugs are widely used clinically. The most targeted molecules in anti-angiogenic therapy fall within two broad categories: VEGF (e.g., bevacizumab targeting VEGFA) and VEGFRs (e.g., cediranib targeting VEGFRs). Bevacizumab, a monoclonal antibody against VEGF, was first approved by the United States Food and Drug Administration for the treatment of metastatic colorectal cancer in 2004. It has shown survival benefits in various solid tumour types, including NSCLC. Bevacizumab not only suppresses tumour growth by reducing neovascularisation and microvessel density (as demonstrated by reduced staining of vascular endothelial cell marker CD31 in tumours) but also activates ICAM-1 and VCAM-1 expression in endothelial cells, thereby recruiting immune cells to the tumour microenvironment [15]. Therefore, we postulate that, in addition to the function of anti-angiogenic agents, the immunomodulatory properties of bevacizumab may also play a role in its clinical activity.

In view of the regulatory effect of the vasculature on the tumour microenvironment, research on the combination of the two has attracted much attention. Combination therapy with atezolizumab, carboplatin, paclitaxel, and bevacizumab has been approved as second-line treatment for patients with advanced NSCLC, and many anti-angiogenic agents and ICI combination therapies are in clinical trials [16]. Preclinical trials of combination therapy have also been conducted in a variety of tumour models and have shown promise. One study showed that anti-VEGFR2 antibody-mediated vascular normalisation can improve immunotherapy by using a low-dose anti-VEGFR2 antibody (DC101) and ICI in a colon cancer model [17]. Similarly, in a mouse model of hepatocellular carcinoma, anti-VEGFR2 antibody-

mediated vascular normalisation improved ICI therapy by reprogramming the immune microenvironment [18]. However, these preclinical models lack the human immune system, which is critical to fully recapitulate the human tumour immune microenvironment. Therefore, they are unable to use antibodies such as pembrolizumab for combination therapy. In recent years, the emergence of humanised immune system mice has brought new hope for preclinical immunotherapy research. Human peripheral blood mononuclear cell (PBMC) and human haematopoietic stem cell (HSC) mouse models were established by transplanting PBMCs or human cord blood-derived CD34 + HSCs into severe combined immunodeficiency mice [19]. Tumour cell lines or patient-derived xenografts were also transplanted into mice. Humanised mouse models are essential for preclinical testing of immunotherapies as they provide insights into the interactions between the human immune system and tumours.

In this study, we hypothesised that bevacizumab may enhance the anti-tumour effect of pembrolizumab by inducing T cell infiltration into tumours without increasing toxicity. To this end, we established a human PBMC (Hu-PBMC) mouse model to conduct combination therapy experiments to investigate the changes in tumour vessels induced by bevacizumab, and determine what effect vascular changes have on tumour-infiltrating immune cells. Our preclinical findings suggest that combination therapy with bevacizumab and pembrolizumab has a synergistic anti-tumour effect, providing a theoretical basis for its first-line clinical application.

Methods

Animal and cell line

Female B-NDG (NOD-Prkdc scid IL2rg tm1/Bcgen) mice (5–6 weeks old) were obtained from Biocytogen (Beijing, China). The mice were maintained under specific pathogen-free conditions and were provided with autoclaved food and water. Mice were humanely euthanised by carbon dioxide inhalation if a solitary subcutaneous tumour exceeded 1,500 mm^3 in size. Animal experiments were performed at the Laboratory Animal Center of the Air Force Military Medical University (Xi'an, China) in accordance with a protocol approved by the Institutional Animal Care and Use Committee (approval number: IACUC-20200602).

The human NSCLC cell lines (H1299 and A549) were purchased from the Cell Bank of the Chinese Academy of Sciences (Shanghai, China). Cells were grown in RPMI-1640 medium (Gibco, Grand Island, NY, USA) supplemented with 10% heat-inactivated foetal bovine serum (Gibco) and 1% penicillin/streptomycin (Thermo Fisher Scientific, Waltham, MA, USA) at 37°C with 5% carbon dioxide. The identity of the cell lines was confirmed by STR profiling (Promega) on an ad hoc basis prior to performing experiments. When 70% confluent, the cells were suspended in serum-free medium with Matrigel (BD Biosciences, San Jose, CA, USA). For *in vivo* studies, 5×10^6 cancer cells were injected subcutaneously into the right flank of humanised mice.

Antibodies

Humanised mice were treated with bevacizumab (anti-VEGF antibody) (Roche, Basel, Switzerland) and pembrolizumab (anti-PD-1 antibody) (Merck, Whitehouse Station, NJ, USA). For flow cytometry, single-cell suspensions were incubated with anti-human CD45-fluorescein isothiocyanate (clone HI30) and anti-human CD3-phycoerythrin (clone UCHT1) antibodies (BD Biosciences). Immunohistochemistry was performed using anti-human CD45 (ab40763; 1:250 dilution), anti-human CD4 (ab133616; 1:500 dilution), and anti-human CD8 (ab108343; 1:400 dilution) antibodies (Abcam, Cambridge, MA, USA). Anti-mouse CD31 (77699; 1:100 dilution) antibodies were purchased from Cell Signalling Technology (Danvers, MA, USA). Immunofluorescence analysis was performed using anti-mouse CD31 (3528; 1:2,000 dilution) (Cell Signalling Technology), anti-human CD45 (ab40763; 1:100 dilution) (Abcam), anti-human CD4 (ab196372; 1:50 dilution) (Abcam), anti-human CD8 (ab237709; 1:100 dilution) (Abcam), anti-mouse ICAM-1 (ab222736; 1:50 dilution) (Abcam), anti-mouse VCAM-1 (ab134047; 1:250 dilution) (Abcam), and anti-mouse alpha-smooth muscle actin (α-SMA) (36110; 1:50 dilution) (Cell Signalling Technology) antibodies. Human CD8 + T cells were depleted by injecting B-NDG mice with human CD8-α monoclonal antibody (clone OKT-T8) (BioXcell, West Lebanon, NH, USA).

Animal experimental protocol

Humanised mice were generated as described previously [19]. Briefly, two fresh peripheral blood samples were collected from the Blood Transfusion Department of Xijing Hospital (Xi'an, China). The protocol was approved by the Medical Ethics Committee (approval number: KY20193035). Whole PBMCs were isolated using Lymphoprep (StemCell Technologies, Vancouver, Canada) according to the manufacturer's instructions. Hu-PBMC mice were generated by intravenous injection of 1×10^7 human PBMCs into 6-week-old female B-NDG mice. The engraftment levels of human CD45 + CD3 + cells were determined 2 weeks after PBMC transplantation by flow cytometric quantification of human peripheral blood CD45 + CD3 + cells. Mice with > 25% human peripheral blood CD45 + CD3 + cells were considered engrafted and humanised. Humanised mice derived from different PBMC donors with diverse levels of human CD45 + CD3 + cells were randomly assigned to each treatment group in each experiment.

Hu-PBMC mice have only a 2–3-week treatment window after successful reconstruction. For optimal use of the treatment window for humanised mice, H1299 or A549 cells were subcutaneously injected into the mice 2 days or 1 week after PBMC transplantation, respectively. In this way, the immune system was successfully constructed 2 weeks later, by which time the initial treatment tumour volume had reached 60–120 mm^3. Tumour size, which was determined every 3–4 days using an electric calliper, was calculated as follows: volume (mm^3) = (length × $width^2$) / 2. Mice were sacrificed when the tumour reached 1,500 mm^3. Five mice per group were used in each animal experiment. Mice with extensive tumour ulceration, weight loss of > 20%, or those that had reached predetermined endpoints were euthanised and excluded from further analysis.

Hu-PBMC cell line-derived xenograft (CDX) mice were treated as follows, with doses determined based on our preliminary experiments and previous studies [20, 21]. In the control group, mice received immunoglobulin G starting 14 days after PBMC transplantation. In the bevacizumab monotherapy group,

bevacizumab (1 mg/kg, intraperitoneally, once every three days) was administered 14 days after PBMC transplantation. In the pembrolizumab monotherapy group, control immunoglobulin G was administered 14 days after PBMC transplantation, followed by pembrolizumab (10 mg/kg, intraperitoneally, once every three days) on day 17. In the combined bevacizumab and pembrolizumab group, bevacizumab was administered 14 days after PBMC transplantation, followed by pembrolizumab on day 17.

Flow cytometry

Two weeks after PBMC transplantation, the peripheral blood of mice was collected from the tail vein to detect the content of humanised level. At the completion of the study, mice were euthanised by carbon dioxide inhalation. Spleen and bone marrow were collected immediately after euthanasia. Mouse PBMCs were incubated with fluorescently labelled antibodies to determine the levels of human CD45 + CD3 + cells in the blood. Cell acquisition was performed using a FC500 flow cytometer (Beckman Coulter, Miami, FL, USA). Data were analysed using FlowJo software (version 10.7) (TreeStar, San Carlos, CA, USA).

Immunohistochemistry and immunofluorescence

Tumours, spleen and bone marrow harvested from humanised mice were fixed in 10% formalin and embedded in paraffin. Tumours were cut into 5 mm sections and subjected to standard haematoxylin and eosin staining or immunohistochemistry. Histology slides were scanned using the Aperio imaging system (Leica Biosystems, Buffalo Grove, IL, USA) and analysed using ImageScope software (Leica Biosystems).

For immunofluorescence analysis, sections were deparaffinised, rehydrated, and boiled in a microwave for 15 min in 10 mM citrate buffer for antigen retrieval. Staining was performed using the aforementioned antibodies. Sections were incubated overnight at 4°C before being incubated with the appropriate Alexa Fluor-conjugated secondary antibodies. The slides were mounted with Fluoroshield/DAPI (Sigma-Aldrich, St. Louis, MO, USA) and imaged using an SP8 confocal microscope (Leica Microsystems, Wetzlar, Germany). For tumour vessel density measurements, immunostained slides were scanned in a low-power field (×40) to identify areas of highest vascularity and then randomly selected within these areas. Tumour vessel density was calculated based on the number of CD31 + luminal structures.

Statistical analysis

All statistical analyses were performed using GraphPad Prism (version 7.0) (GraphPad Software, Inc., San Diego, CA, USA). Data are expressed as means ± standard errors to compare the mean or median values. Differences between groups were tested with ANOVA, and $p < 0.05$ was considered statistically significant.

Results

Combined bevacizumab and pembrolizumab induces synergistic anti-tumour effects in NSCLC irrespective of PD-L1 expression

To investigate the therapeutic effect of the combination of bevacizumab and pembrolizumab, we transplanted human PBMCs and H1299 cells into 27 B-NDG mice to construct humanised mouse model for preclinical efficacy evaluation. When the volume of Hu-PBMC CDX tumour reached 60–120 mm^3, the treatment was commenced and the treatment scheme is illustrated (Fig. 1a). Two weeks later, we monitored the level of human CD45 + CD3 + T cells in the peripheral blood of mice and 20 successfully reconstructed human PBMC CDX mice were divided into four groups: control, bevacizumab monotherapy, pembrolizumab monotherapy, and combined bevacizumab and pembrolizumab (Fig. 1b). Over the course of 14 days, we found that when administered alone, both bevacizumab and pembrolizumab reduced tumour volumes compared to those of untreated mice. Notably, the combination of bevacizumab and pembrolizumab reduced tumour volumes to a greater extent than either of the two monotherapies (Fig. 1c). At the end of treatment, we collected and compared the tumours in each group (Fig. 1d). To evaluate the safety of the combination therapy, the body weight of the mice in each group was dynamically monitored. Graft-versus-host disease resulted in weight loss from about 3 weeks after PBMC transplantation in all groups. However, there was no additional weight loss in mice treated with combination therapy compared to control mice or those treated with bevacizumab or pembrolizumab monotherapy (Fig. 1e).

Furthermore, in order to study whether the effect of the combination therapy was dependent on the level of PD-L1 expression, we also conducted a combination therapy experiment using A549 cell lines, which have low levels of PD-L1 expression. The results showed that pembrolizumab monotherapy was ineffective, while bevacizumab monotherapy and combination therapy could inhibit tumour growth. This suggested that the combination therapy was also effective in treating tumours with low PD-L1 expression (Fig. 1f). Taken together, these results indicate that combination therapy can enhance anti-tumour activity irrespective of PD-L1 expression and with additional toxicity.

Combined bevacizumab and pembrolizumab reprogrammes the tumour immune microenvironment

To analyse the underlying mechanisms of tumour growth inhibition induced by combined PD-1 and VEGF blockade in humanised mice bearing H1299 cells, we first examined the effect of therapy on lymphocyte infiltration using immunohistochemistry (Fig. 2a). Quantitative analysis showed that the number of CD45 + and CD8 + tumour-infiltrating lymphocytes in the combination therapy group was higher than that in the control group. However, there was no significant increase in either of the two monotherapy groups. The numbers of CD4 + T cells were slightly higher in the monotherapy and combination therapy groups than that in the control group, although the difference was not statistically significant (Fig. 2b). As CD8 + T cells are the main mediators of immunotherapy, we further analysed the distribution of CD8 + T cells in the control and combination therapy groups by immunofluorescence staining. In the control group, CD8 + T cells were mainly concentrated at the periphery of the tumour. There was little infiltration in the centre of the tumour, suggesting that the untreated Hu-PBMC CDX model of H1299 cells was of an immune excluded tumour (Fig. 2c). Conversely, CD8 + T cell infiltration was observed both in the centre and at the periphery of the tumour in the combination therapy group (Fig. 2d). This suggests that the combination

of bevacizumab and pembrolizumab can increase the infiltration of immune cells in the centre of the tumour, thereby turning the immune excluded tumour into a ‘hot’ tumour.

Bevacizumab monotherapy and combination therapy promote vascular normalisation

Targeted VEGF therapy can promote vascular normalisation, characterised by decreased microvessel density, increased pericyte coverage, and endothelial cell recovery. We evaluated the effect of combining bevacizumab with pembrolizumab on the tumour vasculature. Tissue sections from each group were stained for the vascular marker CD31 by immunohistochemistry. Bevacizumab alone or in combination with pembrolizumab significantly reduced the total vascular area compared with pembrolizumab alone or control (Fig. 3a). To better define the effect of these therapies on the tumour vasculature, we performed immunofluorescence analysis and measured the vascular area in the centre and at the periphery of the tumour. At the periphery, bevacizumab monotherapy reduced the CD31 + vascular area, whereas the combination of bevacizumab and pembrolizumab resulted in a significantly smaller vascular area compared with that of either monotherapy or control. In the centre, the CD31 + vascular area was reduced in the combination therapy group compared with that of the pembrolizumab monotherapy or control group (Fig. 3b). Next, to assess vascular maturation, pericytes were visualised by α-SMA immunostaining. Consistent with the microvessel density, bevacizumab alone or in combination with pembrolizumab increased pericyte coverage of the surviving tumour vessels, which were mostly found in the stroma or at the periphery of the tumour (Fig. 3c, d). Finally, ICAM-1 and VCAM-1 expression was detected in the endothelial cells of each group to determine whether endothelial cell function had recovered. The proportion of ICAM-1 + CD31 + and VCAM-1 + CD31 + cells in the bevacizumab monotherapy and combination therapy groups was significantly higher than that in the pembrolizumab monotherapy or control group (Fig. 3e, f). Taken together, these results suggest that bevacizumab can promote vascular normalisation.

Reprogramming of the tumour immune microenvironment is mediated by vascular normalisation

A major reason for the formation of immune excluded tumours is that the tumour vasculature inhibits intratumoural lymphocyte extravasation and fosters an immunosuppressive microenvironment, which enables tumours to evade host immunosurveillance. Therefore, we hypothesised that tumour vasculature normalisation may be partially responsible for the different infiltration levels of immune cells between each group. As mentioned above, bevacizumab did not alter the relative abundance of either CD8 + T cells in the tumour microenvironment in the Hu-PBMC CDX model. However, bevacizumab alone or in combination with pembrolizumab increased the absolute numbers of CD8 + T cells specifically in the perivascular space of the tumours, as shown by immunofluorescence staining (Fig. 4a). This suggests that vascular normalisation does increase the infiltration of CD8 + cells around blood vessels. Quantitative morphometric analysis of tumour sections also confirmed these results (Fig. 4c). To further

characterize the extent of altered tumor immunity, we evaluated the activity of intratumoral CD8 + T cells in different treatment settings. CD8 + T cells exhibited significantly increased amounts of Granzyme B proteins in combination groups compared with control (Fig. 4b). Quantitative analysis of each treatment group showed that pembrolizumab monotherapy could also increase the activity of CD8 + T cells (Fig. 4d). These results suggested that both immunotherapy and combination therapy can restore the activity of CD8 + immune cells and therefore kill tumor cells. In order to study whether CD8 + T cells mediate the effect of the combination therapy, we pre-treated humanised mice with anti-CD8 antibody to remove CD8 + T cells *in vivo*, and then administered the combined therapy. The results showed that compared with combined therapy, depletion of CD8 + T cells abrogated the effect of pembrolizumab on bevacizumab therapy (Fig. 4e). Together, these results revealed that bevacizumab therapy could sensitize tumours to pembrolizumab therapy only when sufficient activated cytotoxic CD8 + T cells infiltrated the tumors.

Vascular normalisation improves the tumour microenvironment

Vascular normalisation not only promotes immune cell infiltration but also alters the compactness and oxygen supply in the tumour microenvironment. To evaluate the effect of the combination of bevacizumab and pembrolizumab on solid tumour stress, tumours were stained with haematoxylin and eosin. Tumour cell density was not homogeneous, as demonstrated by the presence of foci of unpacked tumour areas (necrosis areas) surrounded by packed tumour areas (Fig. 5a). Measurements also showed that the tumour necrosis area increased after bevacizumab monotherapy, pembrolizumab monotherapy, and the combination of bevacizumab and pembrolizumab compared with that of the control (Fig. 5b).

Another way to measure improvements in tumour vascular perfusion is to assess tumour oxygenation. To investigate whether vascular normalisation results in changes in tumour oxygenation, we measured hypoxia in Hu-PBMC CDX tumours by immunofluorescence staining of HIF-1α (hypoxia inducible factor-1 α). Tumours from untreated mice were normally oxygenated at the periphery and hypoxic in the centre. Approximately 50% of the total tumour area stained positive for markers of hypoxia. Compared to the control, bevacizumab alone or in combination with pembrolizumab increased zones of oxygenation by 20% and 30%, respectively. An increase in tumour oxygenation supported the hypothesis that the combination of bevacizumab and pembrolizumab can improve tumour vascular perfusion.

Discussion

To the best of our knowledge, this is the first preclinical study to investigate the synergistic anti-tumour effect of the combination of bevacizumab and pembrolizumab *in vivo*. Another preclinical trial [20] showed that targeting VEGF or VEGFR2 can improve the effect of immunotherapy. However, the tumours and antibodies used in these experiments were derived from mice instead of humans, and therefore lack sufficient validity. Numerous ongoing clinical trials urgently need a more relevant preclinical model to explore the theoretical basis of combination therapy [22]. The Hu-PBMC CDX model, which recapitulates

human tumour and human immune system interactions, is an ideal preclinical model for testing novel cancer immunotherapies. To date, humanised mice have been mainly used in the preclinical evaluation of immune checkpoint blockade (ICB) monotherapy, while the application of combination therapy has rarely been reported [23, 24]. Therefore, it is of great significance to explore the therapeutic effect of the combination of bevacizumab and pembrolizumab in a humanised mouse model.

We found that the combination therapy was effective in the treatment of NSCLC regardless of the level of PD-L1 expression and without overt toxicity. This suggests that the addition of bevacizumab has the potential to expand the population benefiting from immunotherapy, while previously only patients with PD-L1 > 50% could receive pembrolizumab treatment. Another factor that should be considered when designing combination therapy is the optimal drug dose and schedule. Our strategy was to first use a low dose of bevacizumab to promote vascular normalisation, followed by ICB therapy 3 days later. A previous study [20] showed that low-dose rather than high-dose anti-VEGFR2 antibodies can promote tumour vasculature normalisation and reprogramme the tumour microenvironment from immunosuppressive to enhance cancer immunotherapy. Notably, high-dose anti-angiogenic therapy can result in a short normalisation window by causing excessive amounts of vessel pruning, thus exacerbating hypoxia and acidosis in the tumour microenvironment [25]. The normalisation process lasts for approximately 1 week in mice and possibly for a few months in humans [26]. Therefore, to achieve the best effect of combination therapy, ICB therapy should be performed during the window of vascular normalisation following anti-VEGF antibody treatment. However, some studies have reported that better results can be achieved by ICB therapy first. [27]. Together, Optimal dose and schedule selection for combined anti-angiogenic and ICB therapy in clinical trials will be critical.

In this study, we found that bevacizumab can reprogramme the immune microenvironment of NSCLC from immune excluded to ‘hot’ tumours. Galon and Bruni [6] categorised tumours into ‘hot’, altered (immune excluded and immunosuppressive), and ‘cold’ tumours according to the distribution of cytotoxic CD3 + and CD8 + T cells in the tumour tissue. They proposed that the immunoscore of tumour tissue is positively correlated with the effect of immunotherapy. Therefore, in NSCLC, the key to the success of immunotherapy-based combination therapy is to convert altered tumours that is devoid of immune effector cells into ‘hot’ tumours by increasing tumour infiltration of T lymphocytes [28]. Farsaci *et al.* [17] found that the combination of anti-angiogenic tyrosine kinase inhibitors and therapeutic vaccines can improve the infiltration level of CD3 + cytotoxic T cells in a colon cancer mouse model. Sanmamed *et al.* [24] also showed that the perivascular accumulation of both CD4 + and CD8 + T cells increased in response to treatment with a combination of angiopoietin-2 and VEGFA inhibition in mouse models of metastatic breast cancer and melanoma. Although the overall number of T cells in the tumour remained unchanged, the anti-cancer activity of the T cells, however, was improved with increased production of interferon-gamma by cytotoxic T lymphocytes. Nevertheless, these studies did not explore changes in the distribution of CD3 + and CD8 + T cells within tumours. Our research shows that bevacizumab can increase the level of CD8 + T cell infiltration both in the centre of the tumour, thereby promoting the therapeutic effect of pembrolizumab.

This study demonstrates that changes in the tumour immune microenvironment are mediated by vascular normalisation. Vascular normalisation can also improve the tumour microenvironment (hypoxia and compactness). This in turn provides a favourable microenvironment for immune cells to become activated and kill tumour cells. Tumour trafficking of activated T cells involves a series of steps, including T cell rolling and adhesion to vascular endothelial cells lining blood vessels. In a previous study [29], angiopoietin-2 and VEGFA inhibition up-regulated the expression of adhesion molecules during the window of vascular normalisation, thereby facilitating the accumulation of T cells in multiple types of mouse tumours. Our study also reported an increase in the formation of mature blood vessels (identified by pericyte coverage), as demonstrated by the increased number of α-SMA + CD31 + vessels.

The immune system of a humanised mouse model constructed using PBMCs is mainly composed of human T cells. Other key immune subpopulations, such as B cells and dendritic cells, are lacking [30]. Therefore, a limitation of this study is that we could not investigate the effect of bevacizumab on these subpopulations and their role in immunotherapy. In subsequent experiments, we used the human HSC B-NDG mouse model constructed using CD34 + HSCs to further study the role of other immune subpopulations in combination therapy.

Conclusions

Taken together, there is an urgent need for novel combination therapies to overcome resistance to single-agent immunotherapies. In this context, our results can be of high translational value since we discuss the rationale for combining immunotherapy with anti-angiogenic treatment. Our study provides powerful preclinical evidence of the effectiveness of bevacizumab in combination with pembrolizumab as first-line therapy for advanced NSCLC.

Abbreviations

α-SMA, alpha-smooth muscle actin; CDX, cell line-derived xenograft; HSC, haematopoietic stem cell; Hu-PBMC, human PBMC; HIF-1α, hypoxia inducible factor-1 α; ICAM-1, intercellular adhesion molecule 1; ICB, immune checkpoint blockade; ICI, immune checkpoint inhibitor; NSCLC, non-small cell lung cancer; PBMC, peripheral blood mononuclear cell; PD-1, programmed death 1; PD-L1, programmed death ligand 1; VCAM-1, vascular cell adhesion molecule 1; VEGF, vascular endothelial growth factor; VEGFR, vascular endothelial growth factor receptor.

Declarations

Ethics approval and consent to participate: All animal experimental procedures were approved by the Institutional Animal Care and Use Committee of the Air Force Military Medical University (Xi'an, China) (approval number: IACUC-20200602) and conducted in accordance with the principles of the 3Rs (replacement, reduction, refinement).

Consent for publication: All animal experimental procedures were performed in compliance with the national regulations on the protection of animals used for scientific purposes and the principles of the 3Rs (replacement, reduction, refinement). All human blood samples were collected after obtaining a written informed consensus from any healthy donor, in accordance with the Declaration of Helsinki.

Availability of data and materials: All data generated or analysed during in this study are included in this published article.

Competing interests: The authors declare that they have no competing interests.

Funding: This work was supported by the National Natural Science Foundation of China (grant number: 81772462).

Authors' contributions: TQ, WG, FM contributed to the conception and design of the study and performed most of the experiments and assisted with manuscript preparation. YZ, YX, YF performed the animal experiments. ZC, YW, JZ, and TJ contributed to the acquisition of data and critically revised the manuscript. CS and YH contributed to the conception of the study and the analysis and interpretation of data and drafted and critically revised the manuscript. All authors gave final approval and agree to be accountable for all aspects of the work.

Acknowledgements: We would like to thank Editage (www.editage.com) for their writing support.

References

1. Bray F, Ferlay J, Soerjomataram I, Siegel RL, Torre LA, Jemal A. Global cancer statistics 2018: GLOBOCAN estimates of incidence and mortality worldwide for 36 cancers in 185 countries. CA Cancer J Clin. 2018;68:394–424.
2. Miller KD, Nogueira L, Mariotto AB, Rowland JH, Yabroff KR, Alfano CM, et al. Cancer treatment and survivorship statistics, 2019. CA Cancer J Clin. 2019;69:363–85.
3. Kas B, Talbot H, Ferrara R, Richard C, Lamarque JP, Pitre-Champagnat S, et al. Clarification of definitions of hyperprogressive disease during immunotherapy for non-small cell lung cancer. JAMA Oncol. 2020;6:1039–46.
4. Rotte A. Combination of CTLA-4 and PD-1 blockers for treatment of cancer. J Exp Clin Cancer Res. 2019;38:255.
5. Brahmer JR. Harnessing the immune system for the treatment of non-small-cell lung cancer. J Clin Oncol. 2013;31:1021–8.
6. Galon J, Bruni D. Approaches to treat immune hot, altered and cold tumours with combination immunotherapies. Nat Rev Drug Discov. 2019;18:197–218.
7. Hegde PS, Chen DS. Top 10 challenges in cancer immunotherapy. Immunity. 2020;52:17–35.
8. Fang L, Ly D, Wang SS, Lee JB, Kang H, Xu H, et al. Targeting late-stage non-small cell lung cancer with a combination of DNT cellular therapy and PD-1 checkpoint blockade. J Exp Clin Cancer Res.

2019;38:123.
9. Ricciuti B, Foglietta J, Bianconi V, Sahebkar A, Pirro M. Enzymes involved in tumor-driven angiogenesis: A valuable target for anticancer therapy. Semin Cancer Biol. 2019;56:87–99.
10. Hosaka K, Yang Y, Seki T, Du Q, Jing X, He X, et al. Therapeutic paradigm of dual targeting VEGF and PDGF for effectively treating FGF-2 off-target tumors. Nat Commun. 2020;11:3704.
11. Lee DH, Lee MY, Seo Y, Hong HJ, An HJ, Kang JS, et al. Multi-paratopic VEGF decoy receptor have superior anti-tumor effects through anti-EGFRs and targeted anti-angiogenic activities. Biomaterials. 2018;171:34–45.
12. Rahbari NN, Kedrin D, Incio J, Liu H, Ho WW, Nia HT, et al. Anti-VEGF therapy induces ECM remodeling and mechanical barriers to therapy in colorectal cancer liver metastases. Sci Transl Med. 2016;8:360ra135.
13. Hendry SA, Farnsworth RH, Solomon B, Achen MG, Stacker SA, Fox SB. The role of the tumor vasculature in the host immune response: implications for therapeutic strategies targeting the tumor microenvironment. Front Immunol. 2016;7:621.
14. Kim I, Moon SO, Park SK, Chae SW, Koh GY. Angiopoietin-1 reduces VEGF-stimulated leukocyte adhesion to endothelial cells by reducing ICAM-1, VCAM-1, and E-selectin expression. Circ Res. 2001;89:477–9.
15. Liu Y, Starr MD, Brady JC, Rushing C, Pang H, Adams B, et al. Modulation of circulating protein biomarkers in cancer patients receiving bevacizumab and the anti-endoglin antibody, TRC105. Mol Cancer Ther. 2018;17:2248–56.
16. Reck M, Wehler T, Orlandi F, Nogami N, Barone C, Moro-Sibilot D, et al. Safety and patient-reported outcomes of atezolizumab plus chemotherapy with or without bevacizumab versus bevacizumab plus chemotherapy in non-small-cell lung cancer. J Clin Oncol. 2020;38:2530–42.
17. Farsaci B, Donahue RN, Coplin MA, Grenga I, Lepone LM, Molinolo AA, et al. Immune consequences of decreasing tumor vasculature with antiangiogenic tyrosine kinase inhibitors in combination with therapeutic vaccines. Cancer Immunol Res. 2014;2:1090–102.
18. Shigeta K, Datta M, Hato T, Kitahara S, Chen IX, Matsui A, et al. Dual programmed death receptor-1 and vascular endothelial growth factor receptor-2 blockade promotes vascular normalization and enhances antitumor immune responses in hepatocellular carcinoma. Hepatology. 2020;71:1247–61.
19. Meraz IM, Majidi M, Meng F, Shao R, Ha MJ, Neri S, et al. An improved patient-derived xenograft humanized mouse model for evaluation of lung cancer immune responses. Cancer Immunol Res. 2019;7:1267–79.
20. Huang Y, Yuan J, Righi E, Kamoun WS, Ancukiewicz M, Nezivar J, et al. Vascular normalizing doses of antiangiogenic treatment reprogram the immunosuppressive tumor microenvironment and enhance immunotherapy. Proc Natl Acad Sci U S A. 2012;109:17561–6.
21. Jain RK. Antiangiogenesis strategies revisited: from starving tumors to alleviating hypoxia. Cancer Cell. 2014;26:605–22.

22. Gao F, Yang C. Anti-VEGF/VEGFR2 monoclonal antibodies and their combinations with PD-1/PD-L1 inhibitors in clinic. Curr Cancer Drug Targets. 2020;20:3–18.
23. De La Rochere P, Guil-Luna S, Decaudin D, Azar G, Sidhu SS, Piaggio E. Humanized mice for the study of immuno-oncology. Trends Immunol. 2018;39:748–63.
24. Sanmamed MF, Rodriguez I, Schalper KA, Onate C, Azpilikueta A, Rodriguez-Ruiz ME, et al. Nivolumab and urelumab enhance antitumor activity of human T lymphocytes engrafted in Rag2–/– IL2Rγnull immunodeficient mice. Cancer Res. 2015;75:3466–78.
25. Griveau A, Seano G, Shelton SJ, Kupp R, Jahangiri A, Obernier K, et al. A glial signature and Wnt7 signaling regulate glioma-vascular interactions and tumor microenvironment. Cancer Cell. 2018;33:874–89.
26. Batchelor TT, Sorensen AG, di Tomaso E, Zhang WT, Duda DG, Cohen KS, et al. AZD2171, a pan-VEGF receptor tyrosine kinase inhibitor, normalizes tumor vasculature and alleviates edema in glioblastoma patients. Cancer Cell. 2007;11:83–95.
27. Lai X, Friedman A. How to schedule VEGF and PD-1 inhibitors in combination cancer therapy? BMC Syst Biol. 2019;13:30.
28. Pan C, Liu H, Robins E, Song W, Liu D, Li Z, et al. Next-generation immuno-oncology agents: current momentum shifts in cancer immunotherapy. J Hematol Oncol. 2020;13:29.
29. Fukumura D, Kloepper J, Amoozgar Z, Duda DG, Jain RK. Enhancing cancer immunotherapy using antiangiogenics: opportunities and challenges. Nat Rev Clin Oncol. 2018;15:325–40.
30. Verma B, Wesa A. Establishment of humanized mice from peripheral blood mononuclear cells or cord blood CD34 + hematopoietic stem cells for immune-oncology studies evaluating new therapeutic agents. Curr Protoc Pharmacol. 2020;89:e77.

Figures

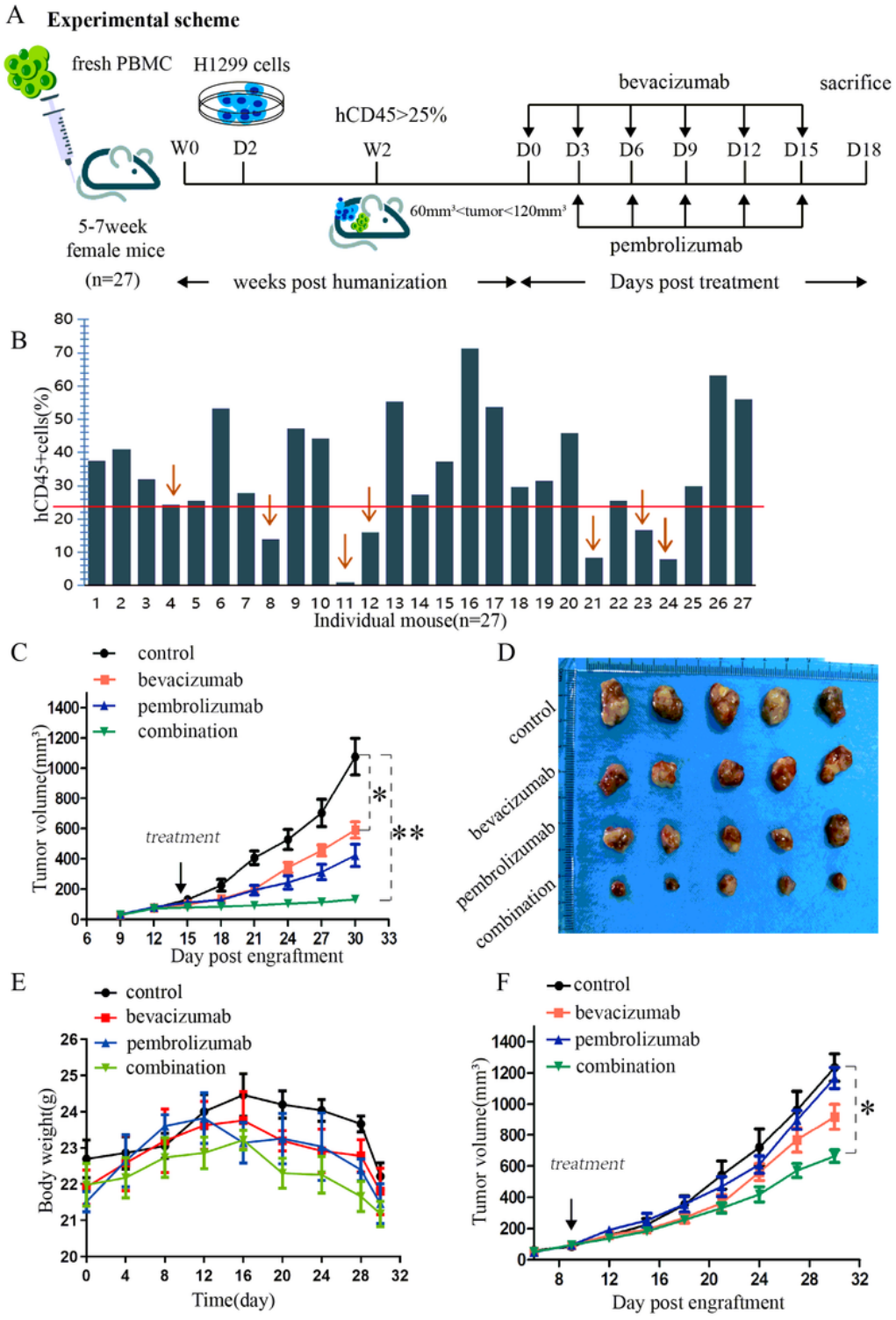

Figure 1

Efficacy of combined bevacizumab and pembrolizumab in humanised mouse models of non-small cell lung cancer. (a) Schematic diagram of the construction and treatment of humanised mice. Adult B-NDG mice were injected with 1 × 107 peripheral blood mononuclear cells intravenously, followed by subcutaneous injection of 5 × 106 tumour cell lines. After 2 weeks, the mice were randomly assigned to each treatment group. (b) In the second week of PBMCs transplantation, the level of human

CD45+CD3+T cells in the peripheral blood of mice was monitored by flow cytometry, and the mice with a reconstruction level of more than 25% were selected for follow-up experiments. (c) Tumour growth curves of humanised mice bearing H1299 cells in the control, bevacizumab monotherapy, pembrolizumab monotherapy, and combination therapy groups. Data are presented as the mean ± standard deviation of the cell line-derived xenograft volume (mm3) (n = 5). *P < 0.05, **P < 0.01, and ***P < 0.001. (d) At the end of treatment, the tumours were collected and photographed. (e) The body weight of the mice in each treatment group was monitored every 4 days from the beginning of peripheral blood mononuclear cell transplantation to the end of treatment (n = 5). (f) Tumour growth curves of humanised mice bearing A549 cells in each of the four treatment groups. Data are presented as the mean ± standard deviation of the cell line-derived xenograft volume (mm3) (n = 5). Statistically significant differences at day 30 after PBMC transplant, based on ANOVA. *P < 0.05, **P < 0.01, and ***P < 0.001.

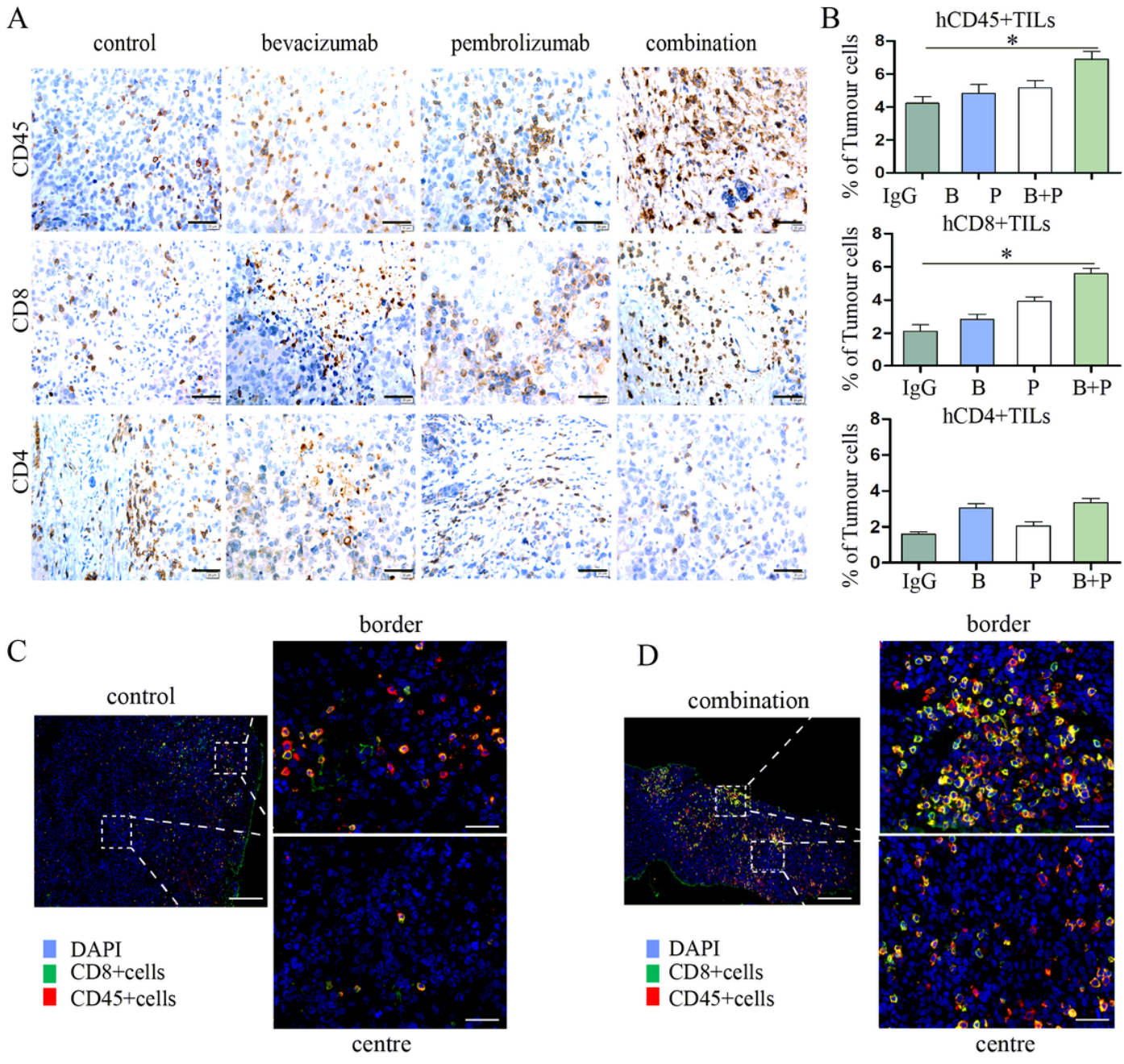

Figure 2

The impact of combined bevacizumab and pembrolizumab on the tumour immune microenvironment. (a) Immunohistochemical staining of CD45+, CD4+, and CD8+ cells in tumours treated as indicated. Representative images were taken at ×40 magnification. The scale bar denotes 20 μm. (b) Quantification of CD45+, CD4+, and CD8+ cells in H1299 tumours treatment with IgG, bevacizumab (B), pembrolizumab (P), and combination therapy (B + P). Each number indicates one tumour per mouse and represents the average of 5 images (n = 5). Statistically significant differences based on ANOVA. *P < 0.05, **P < 0.01, and ***P < 0.001. (c–d) Immunofluorescence analysis of the distribution of CD45+ T cells (red) and CD8+ T cells (green) in the centre and at the periphery of tumour tissue in the control and combination therapy groups. Scale bars, 200 μm (low-magnification images); 20 μm (high-magnification images).

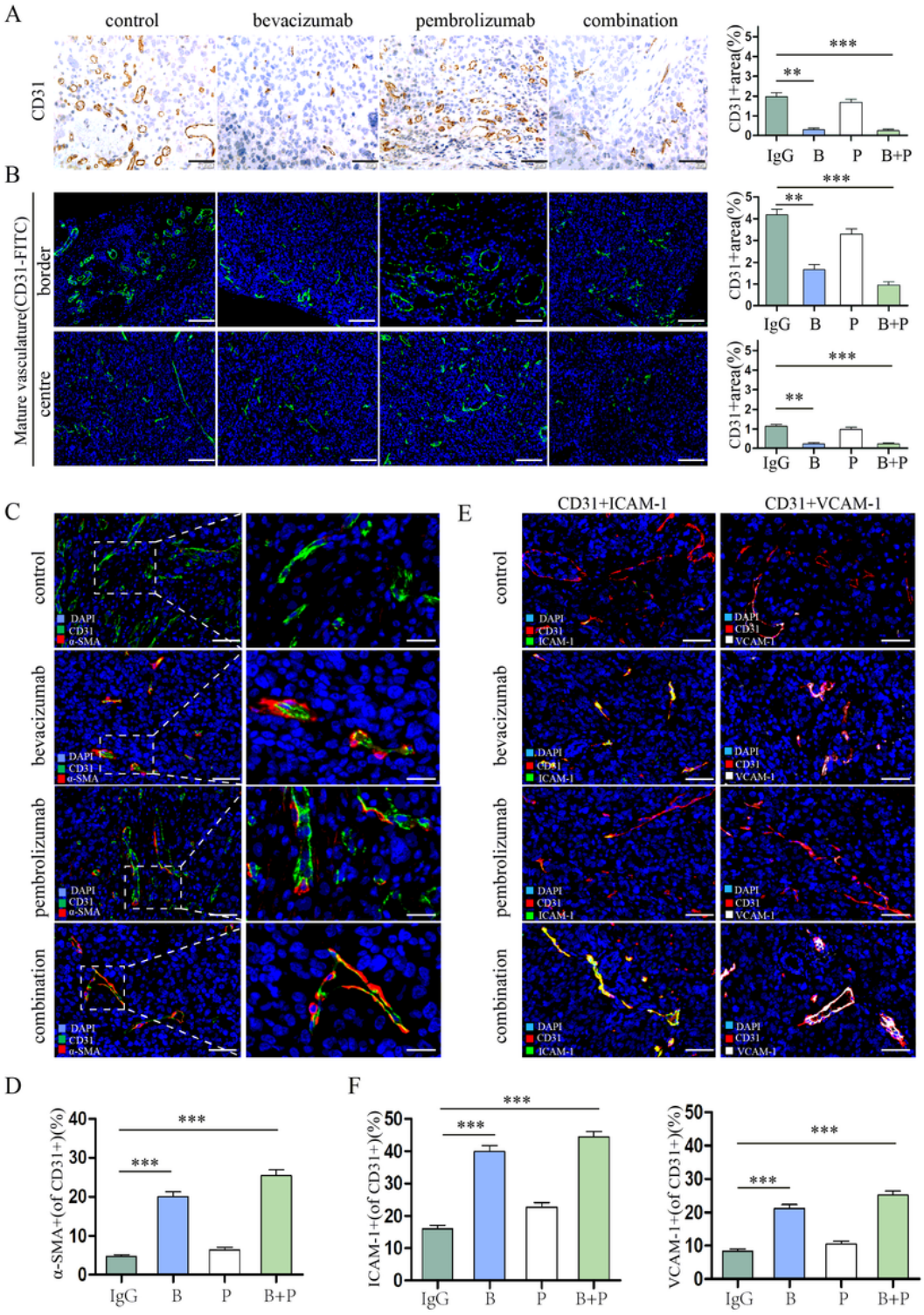

Figure 3

Bevacizumab monotherapy and combination therapy promote vascular normalisation. (a) Immunohistochemical analysis and quantification of CD31+ areas in tumours. Representative images were taken at ×40 magnification. The scale bar denotes 20 μm. Each number indicates one tumour per mouse and represents the average of 5 images (n = 5). (b) Immunofluorescence analysis and quantification of CD31+ areas in the centre and at the periphery of tumours treated as indicated.

Representative images of CD31 immunostaining (green) and DAPI nuclear staining (blue) of tumours. Scale bars denote 50 μm. Each number indicates one tumour per mouse and represents the average of 5 images (n = 5). (c) Representative images of CD31+ (green) and α-smooth muscle actin (α-SMA)+ (red) immunostaining and DAPI nuclear staining (blue) of tumours treated as indicated. Scale bars, 20 μm (low-magnification images). Relative proportion of α-SMA+ pericyte-covered blood vessels in tumours treated as indicated. Each number indicates one tumour per mouse and represents the average of 5 images (n = 5). (d) Representative images of CD31+ (green) and intercellular adhesion molecule 1 (ICAM-1)+ (red)/vascular cell adhesion molecule 1 (VCAM-1)+ (white) immunostaining and DAPI nuclear staining (blue) of tumours treated as indicated. Scale bars denote 20 μm. Relative proportion of ICAM-1+/VCAM-1+ blood vessels in tumours treated as indicated. Each number indicates one tumour per mouse and represents the average of 5 images (n = 5). Statistically significant differences based on ANOVA. *P < 0.05, **P < 0.01, and ***P < 0.001.

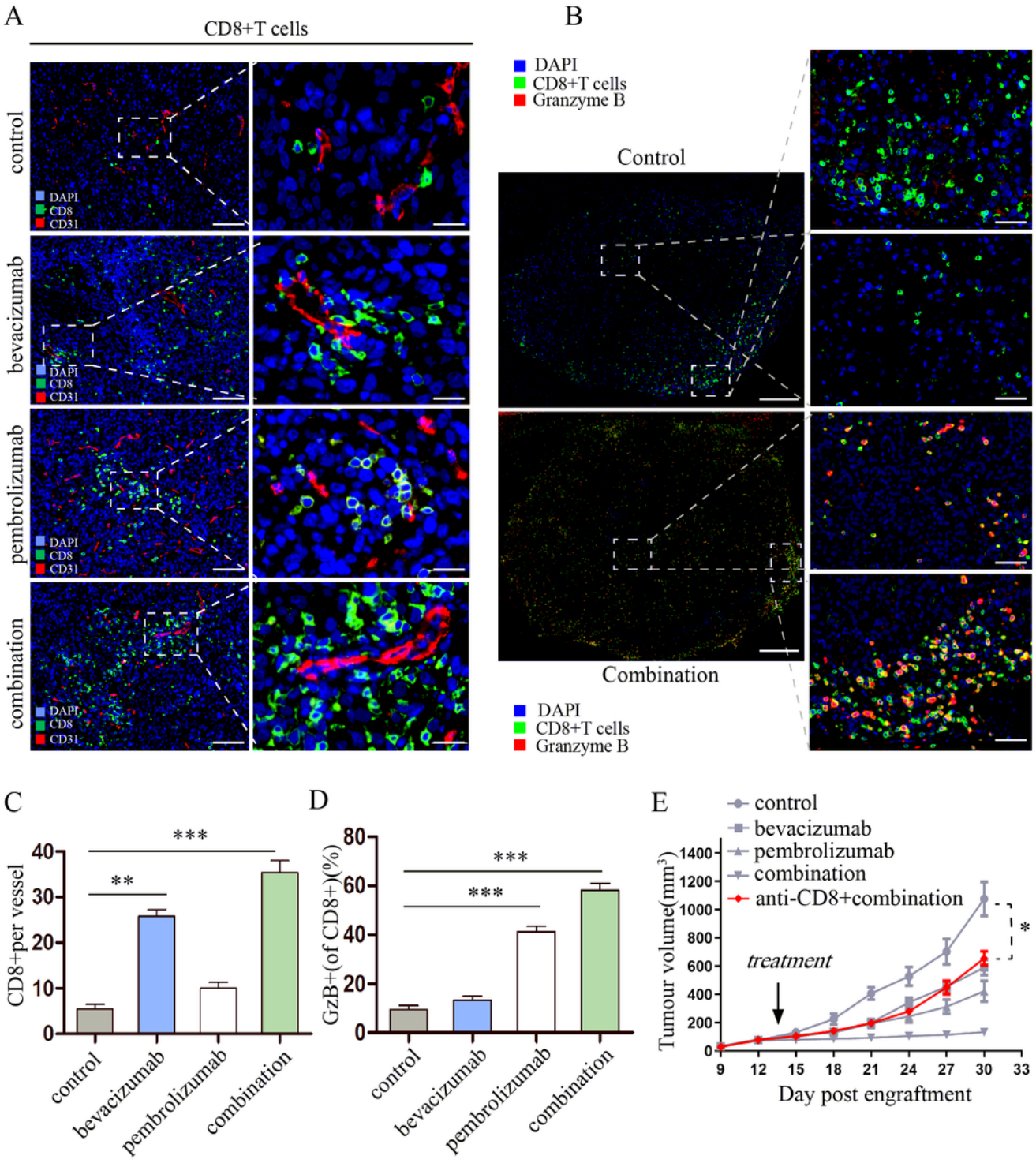

Figure 4

Combined bevacizumab and pembrolizumab promotes extravasation and perivascular accumulation of CD8+ T cells in tumours. (a) Representative images of CD8+ (green) and CD31+ (red) immunostaining and DAPI nuclear staining (blue) in tumours treated as indicated. Scale bars, 50 μm (low-magnification images). (b) Visualization of Granzyme B+ CD8+ T cells in tumors treated with IgG or combination groups. (c) Quantification of perivascular CD8+ T cells in tumours treated as indicated. Each number

indicates one tumour per mouse and represents the average of 5 images (n = 5). Statistically significant differences based on ANOVA. (d) Quantitation of Granzyme B+ CD8+ T cells in tumors treated as indicated. (e) Tumour growth curves of H1299 tumours treated with before-mentioned four groups and anti-CD8-depleting monoclonal antibody combination with bevanizumab + pembrolizumab (B + P). The results showed that the effect of combined therapy depended on CD8+ T cells. Data are presented as the mean ± standard deviation of the cell line-derived xenograft volume (mm3) (n = 5). Statistically significant differences at day 30 after PBMC transplant, based on ANOVA. *P < 0.05 and **P < 0.01.

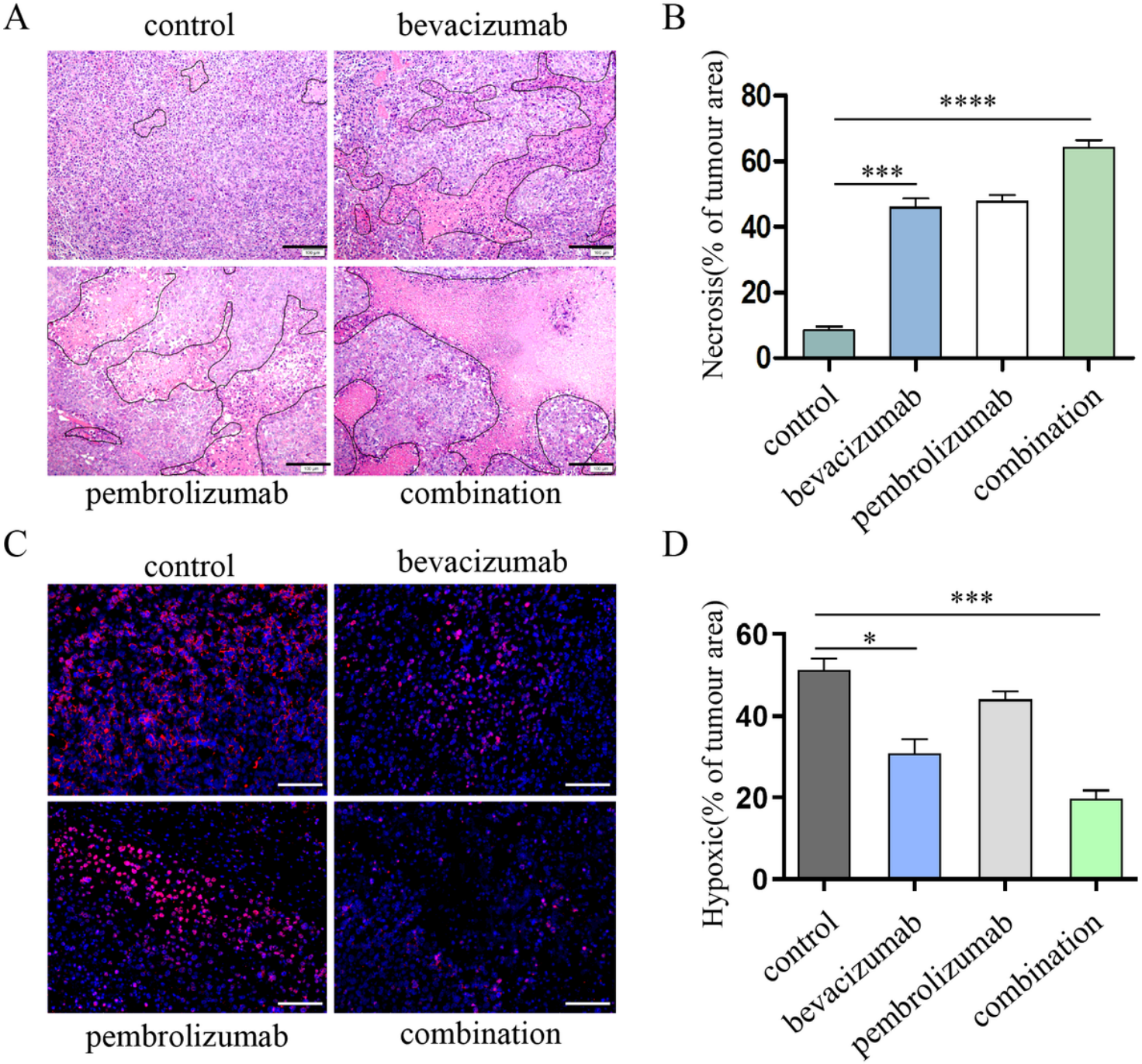

Figure 5

Combined bevacizumab and pembrolizumab affects the pressure and oxygen supply in the tumour microenvironment. (a–b) Effect of bevacizumab, pembrolizumab, and their combination on tumour compactness. Haematoxylin and eosin stained tumour sections at ×10 magnification show tumour compactness. Less compact areas are outlined in black and their relative proportion was quantified. Each dot indicates one tumour per mouse and represents the average of 5 images. Statistically significant differences based on ANOVA (n = 5). *P < 0.05 and **P < 0.01. (c–d) Immunofluorescence labelling of hypoxia-inducible factor 1 was used to evaluate the oxygen supply to the tumour. Scale bars denote 50 μm. Quantification of hypoxia areas was conducted to evulated the oxygen supply between each groups.

Supplementary Files

This is a list of supplementary files associated with this preprint. Click to download.

- Additionalfile1.pdf
- Additionalfile2.pdf
- Additionalfile3.pdf